J. Fluid Mech. (2010), *vol.* 657, *pp.* 265–284.
doi:10.1017/S002211201000145X

The rise and fall of turbulent fountains: a new model for improved quantitative predictions

G. CARAZZO[1]†, E. KAMINSKI[2] AND S. TAIT[2]

[1]Department of Earth and Ocean Sciences, The University of British Columbia, 6338 Stores Rd, Vancouver, BC, Canada V6T 1Z4

[2]Equipe de Dynamique des Fluides Géologiques, Université Paris Diderot and Institut de Physique du Globe de Paris, 4 place Jussieu, 75252 Paris CEDEX 05, France

(Received 9 September 2009; revised 4 March 2010; accepted 17 March 2010; first published online 10 June 2010)

Turbulent fountains are of major interest for many natural phenomena and industrial applications, and can be considered as one of the canonical examples of turbulent flows. They have been the object of extensive experimental and theoretical studies that yielded scaling laws describing the behaviour of the fountains as a function of source conditions (namely their Reynolds and Froude numbers). However, although such scaling laws provide a clear understanding of the basic dynamics of the turbulent fountains, they usually rely on more or less *ad hoc* dimensionless proportionality constants that are scarcely tested against theoretical predictions. In this paper, we use a systematic comparison between the initial and steady-state heights of a turbulent fountain predicted by classical top-hat models and those obtained in experiments. This shows scaling agreement between predictions and observations, but systematic discrepancies regarding the proportionality constant. For the initial rise of turbulent fountains, we show that quantitative agreement between top-hat models and experiments can be achieved by taking into account two factors: (i) the reduction of entrainment by negative buoyancy (as quantified by the Froude number), and (ii) the fact that turbulence is not fully developed at the source at intermediate Reynolds number. For the steady-state rise of turbulent fountains, a new model ('confined top-hat') is developed to take into account the coupling between the up-flow and the down-flow in the steady-state fountain. The model introduces three parameters, calculated from integrals of experimental profiles, that highlight the dynamics of turbulent entrainment between the up-flow and the down-flow, as well as the change of buoyancy flux with height in the up-flow. The confined top-hat model for turbulent fountains achieves good agreement between theoretical predictions and experimental results. In particular, it predicts a systematic increase of the ratio between the initial and steady-state heights of turbulent fountains as a function of their source Froude number, an observation that was not handled properly in previous models.

Key words: mixing and dispersion, modelling, theory

1. Introduction

A turbulent fountain is created when dense fluid is ejected upwards (or light fluid downwards) into a less (more) dense environment (Turner 1966). Turbulent fountains

† Email address for correspondence: gcarazzo@eos.ubc.ca

are of particular importance in various natural and industrial processes such as the replenishment of magma chambers (Campbell & Turner 1989), cumulonimbus convection in the atmosphere (McDougall 1981), explosive volcanic eruptions (Branney & Kokelaar 1992), refuelling compensated fuel tanks on naval vessels (Friedman *et al.* 2007), waste disposal systems (Koh & Brooks 1975) or heating and ventilation of large buildings (Baines, Turner & Campbell 1990). They also feature amongst canonical turbulent flows (Linden 2000). Turbulent fountains have been widely studied and their basic dynamics are well described experimentally: they are characterized by an initial stage during which the starting jet decelerates due both to the entrainment of surrounding fluid and to the negative buoyancy force. When the velocity falls to zero at some initial height z_m, the flow reverses direction and falls back as an annular plume around the up-flowing fountain core. At steady state, the turbulent interaction between the up-flow and the down-flow reduces the height initially reached by the fountain which fluctuates around a final mean value, z_{ss}. It has become common in the literature to characterize the dynamics of turbulent fountains by relationships between the initial or steady-state heights and the Reynolds ($Re_0 = w_0 R_0/\nu$) and Froude ($Fr_0 = w_0/\sqrt{R_0|g_0'|}$) numbers, where the subscript '0' denotes source values and w, R, ν and $g' = g(\rho_e - \rho_0)/\rho_e$ are the upward velocity, the flow radius, the kinematic viscosity and the reduced gravity with ρ_0 and ρ_e the density of the flow and the environment, respectively.

Different studies have focused on the behaviour of fountains with various geometries: round (Turner 1966; McDougall 1981; Baines *et al.* 1990; Cresswell & Szczepura 1993; Zhang & Baddour 1998; Bloomfield & Kerr 2000; Lin & Armfield 2000*a*; Philippe *et al.* 2005; Kaye & Hunt 2006; Williamson *et al.* 2008), planar (Turner 1966; Campbell & Turner 1989; Baines *et al.* 1990; Zhang & Baddour 1997; Hunt & Coffey 2009) or impinging on a density interface (Cotel *et al.* 1997; Lin & Linden 2005; Friedman 2006; Friedman *et al.* 2007; Ansong, Kyba & Sutherland 2008). In most of the experiments investigated, the Reynolds number of the flow is high and the general behaviour of the fountain is controlled by the source Froude number. The typical scaling is then $z_m/R_0 \sim {Fr_0}^p$, where different values of p apply in different ranges of values of Fr_0. Based on theoretical analysis and laboratory experiments Kaye & Hunt (2006) suggest that $p = 2/3$ for low-Froude-number fountains ($Fr_0 < 1$) and $p = 2$ for intermediate Froude number ($1 < Fr_0 < 10$). The experiments of Zhang & Baddour (1998) implied that $p = 1.3$, whereas the numerical simulations of Lin & Armfield (2004, 2008) showed a dependence on the source Reynolds number ${Re_0}^{1/4}$, with $p = 1$ (Lin & Armfield 2004) and $p = 3/2$ (Lin & Armfield 2008). At high Froude number, the analysis and the laboratory experiments of Turner (1966), Baines *et al.* (1990), Zhang & Baddour (1998) and Kaye & Hunt (2006) converge to the conclusion that z_m/R_0 scales with Fr_0. At low source Reynolds number, the flow is laminar and the maximum height reached by a round fountain may follow the scaling $z_m/R_0 \sim Fr_0 {Re_0}^n$, where the value for n has been debated. Numerical simulations of low-Froude-number laminar fountains ($Fr_0 < 1$) suggest that $n = -2/3$ (Lin & Armfield 2000*b*), $n = 0$ (Lin & Armfield 2000*a*) or $n = -1/2$ (Lin & Armfield 2003). For higher source Froude number ($Fr_0 > 1$), the laboratory experiments of Philippe *et al.* (2005) and Williamson *et al.* (2008) agreed on $n = 1/2$.

Previous studies mainly focused on describing the different dynamical regimes of the fountain as a function of the conditions imposed at the source, in order to determine scaling laws for the maximum (initial) and the steady-state heights. Such scaling laws come from theoretical models for turbulent flows, namely top-hat models inspired by the work of Morton, Taylor & Turner (1956), that can be used to obtain

analytical exact solutions for the rise of turbulent fountains. Based on a careful review of experimental data from the literature, we show in this paper that the analytical solution does not agree with those measured in the laboratory experiments. Such a discrepancy is all the more problematic for the quantitative prediction of large-scale flow behaviour like that of explosive volcanic fountains. These powerful natural flows which are too dangerous to permit detailed observations require an accurate physical description to infer exit conditions from the maximum height reached above the vent. The aim of this paper is to discuss and eventually correct this discrepancy. For this, we propose to take into account the effect of buoyancy on turbulent entrainment and we develop a new top-hat model for a steady-state fountain.

2. Previous work: scaling laws and their predictions

During the initial ascent phase of a highly forced fountain, the flow behaves like a jet and entrains surrounding fluid (Bloomfield & Kerr 2000; Kaye & Hunt 2006; Hunt & Coffey 2009). This first rising flow can thus be modelled in the Boussinesq approximation with the conservation equations of Morton *et al.* (1956):

$$\frac{\mathrm{d}}{\mathrm{d}z}(WR^2) = 2\alpha_e WR, \tag{2.1}$$

$$\frac{\mathrm{d}}{\mathrm{d}z}(W^2R^2) = G'R^2, \tag{2.2}$$

$$\frac{\mathrm{d}}{\mathrm{d}z}(G'WR^2) = 0, \tag{2.3}$$

where z is the distance from the source and πWR^2, πW^2R^2 and $\pi G'WR^2$ are the volume, momentum and buoyancy fluxes, respectively. The entrainment coefficient α_e quantifies the entrainment rate $\alpha_e W$. These equations are valid for self-similar flows. Although laboratory measurements of velocity and buoyancy profiles do not fully support this assumption at any distance from the source (Mizushina *et al.* 1982; Cresswell & Szczepura 1993), this model has been successfully applied to turbulent fountains (Bloomfield & Kerr 2000). Hunt & Kaye (2005) and Kaye & Hunt (2006) solved for the dimensionless form of these equations and obtained the following scaling law at large Froude number ($Fr_0 > 3$):

$$\frac{z_m}{R_0} = 0.865\,\alpha_e^{-1/2} Fr_0. \tag{2.4}$$

The prediction $z_m/R_0 \sim Fr_0$ was compared successfully to experiments in Kaye & Hunt (2006). However, the value of the proportionality constant ($0.865\,\alpha_e^{-1/2}$) has not been thoroughly tested yet.

Figure 1 compares laboratory measurements of dimensionless maximum heights (Zhang & Baddour 1998; Bloomfield & Kerr 2000; and the present study) with the model of Morton *et al.* (1956) (defined in (2.1)–(2.3)) using $\alpha_e = 0.1$ as a reference value for the entrainment coefficient (Kaye & Hunt 2006) or $0.865\,\alpha_e^{-1/2} = 2.735$ as proportionality constant in the scaling law (2.4). The maximum heights predicted by the model are consistent with the scaling law in terms of dependence on Fr_0, but the predictions are systematically smaller than the experimental values. In other words, the experimental value of the effective entrainment coefficient in relation (2.4) is smaller than the value $\alpha_e = 0.1$ used in the analytical solution.

The prediction of the steady-state height reached by a turbulent fountain is usually handled by using the predictions of the initial maximum height corrected with the

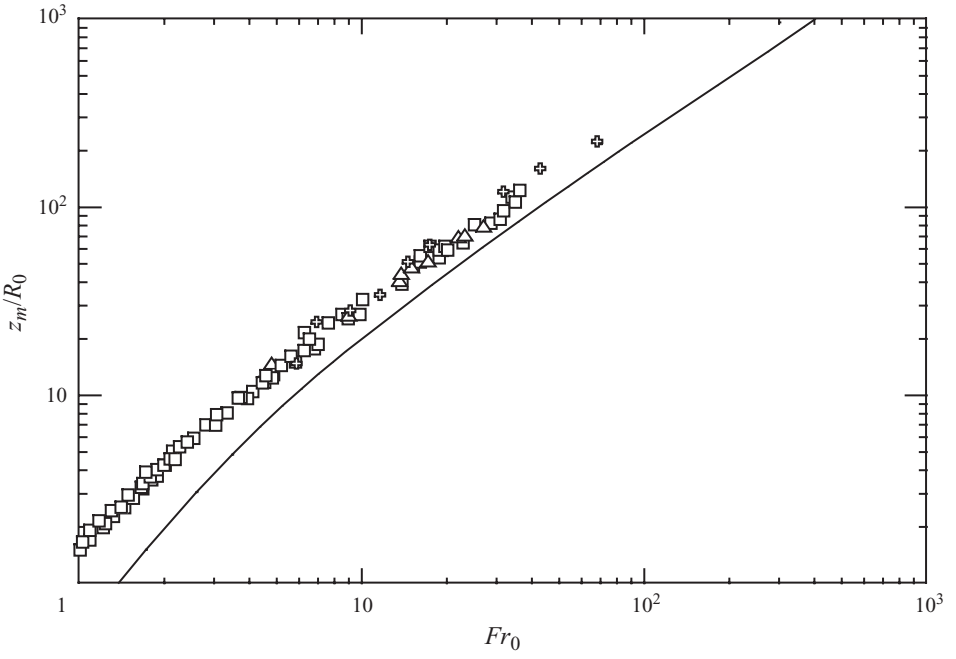

FIGURE 1. Dimensionless maximum rise height (z_m/R_0) of experimental fountains as a function of the source Froude number compared with the theoretical predictions (solid line) using the model of Morton *et al.* (1956) with $\alpha_e = 0.1$. △, Zhang & Baddour (1998); □, Bloomfield & Kerr (2000); ✣, the present study (see the Appendix). Error bars are smaller than the symbol size.

factor $z_m/z_{ss} = 1.43$ determined experimentally by Turner (1966). Figure 2 shows the comparison between theoretical predictions for z_{ss} obtained using $z_m/z_{ss} = 1.43$ and z_m from relation (2.4), and laboratory measurements. Here again, although experimental values follow the theoretical scaling, there is a large discrepancy. Such a discrepancy may reflect a wrong estimate of z_{ss} through inappropriate use of a fixed z_m/z_{ss} ratio of 1.43, as well as the fact that 0.1 may be an inadequate value for the entrainment coefficient α_e in the model. Recent studies have shown indeed that for highly forced fountains $\alpha_e \sim \alpha_{jet}$, whereas for weak and very weak fountains the height reached is independent of the choice of α_e (Kaye & Hunt 2006; Hunt & Coffey 2009). We thus propose to relax these hypotheses of fixed z_m/z_{ss} and α_e in a new model of turbulent fountains.

3. Quantitative prediction of maximum (initial) height

Recent papers (Kaminski, Tait & Carazzo 2005; Carazzo, Kaminski & Tait 2006; Papanicolaou, Papakonstantis & Christodoulou 2008) demonstrated that entrainment in turbulent jets is reduced by negative buoyancy. Such an effect modifies the dynamics of turbulent fountains as their specific dynamics is due to negative buoyancy. The effect of buoyancy on entrainment can be quantified using the formalism developed in two companion papers by Kaminski *et al.* (2005) and Carazzo *et al.* (2006). In this model, the rate of entrainment depends on the amount and sign of the buoyancy, and on the local shapes of the velocity, buoyancy and turbulent stress profiles. The

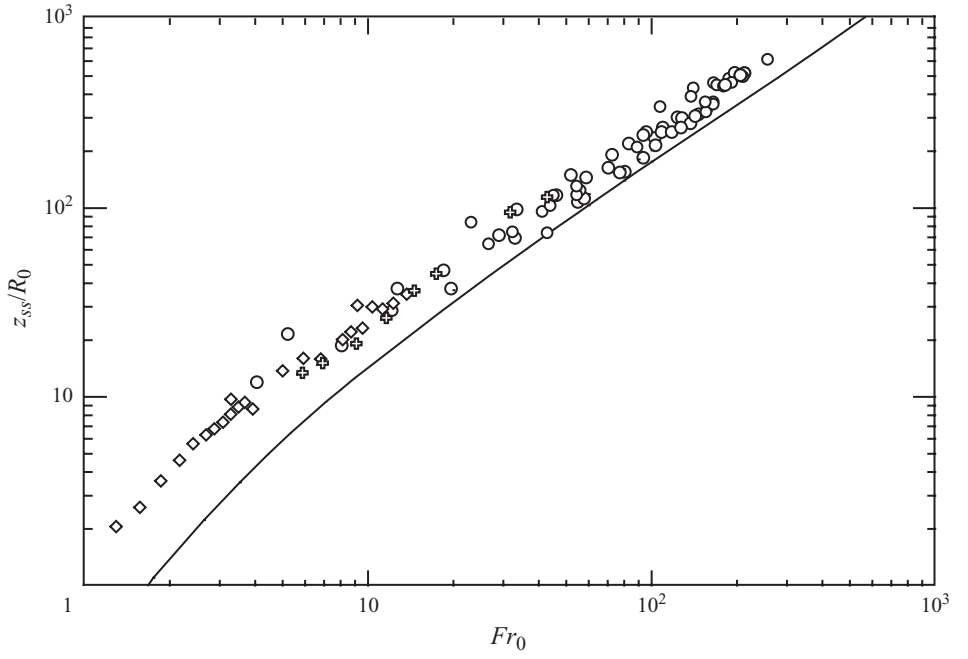

FIGURE 2. Dimensionless steady-state height (z_{ss}/R_0) of experimental fountains as a function of the source Froude number compared with theoretical predictions (solid line) using the model of Morton *et al.* (1956) with $\alpha_e = 0.1$ and using $z_m/z_{ss} = 1.43$ as in Kaye & Hunt (2006). ○, Baines *et al.* (1990); ◇, Kaye & Hunt (2006); ✣, the present study (see the Appendix). Error bars are smaller than the symbol size.

resulting explicit expression for the variable entrainment coefficient is

$$\alpha_e = \frac{C}{2} + \left(1 - \frac{1}{A}\right) Ri + \frac{R}{2}\frac{\mathrm{d}\ln A}{\mathrm{d}z}, \tag{3.1}$$

where $Ri = G'R/W^2 \equiv \mathrm{sign}\,(G')\,1/Fr^2$ is the Richardson number, which is negative in the case of fountains discussed here. Note that the Richardson number is similar to the source parameter Γ defined by Morton (1959) but not strictly the same as it does not involve α_e. A and C are dimensionless parameters that are functions of the shapes of the cross-stream profiles of velocity, reduced gravity and turbulent stress. For example, in the case of Gaussian velocity and buoyancy profiles, A and C are given by

$$A = \tfrac{2}{3}(1 + \lambda^2), \tag{3.2}$$

$$C = -6(1 + \lambda^2)\int_0^\infty r^* \exp(-r^{*^2})\, j(r^*)\,\mathrm{d}r^*, \tag{3.3}$$

where λ is the ratio of the characteristic $(1/e)$ width of the buoyancy profile (δ_c) to that of the velocity profile (δ_w), j is the turbulent shear stress profile and $r^* = r/\delta_w$. A and C have been constrained at large distance from the source by various experimental constraints (Carazzo *et al.* 2006; Carazzo, Kaminski & Tait 2008*a*). C, which represents the fraction of the total energy flux available for entrainment (Kaminski *et al.* 2005), was found to be a constant equal to 0.135, whereas A varies from 1.1 to 1.8 as a function of distance from source and of the characteristics of the jet (pure

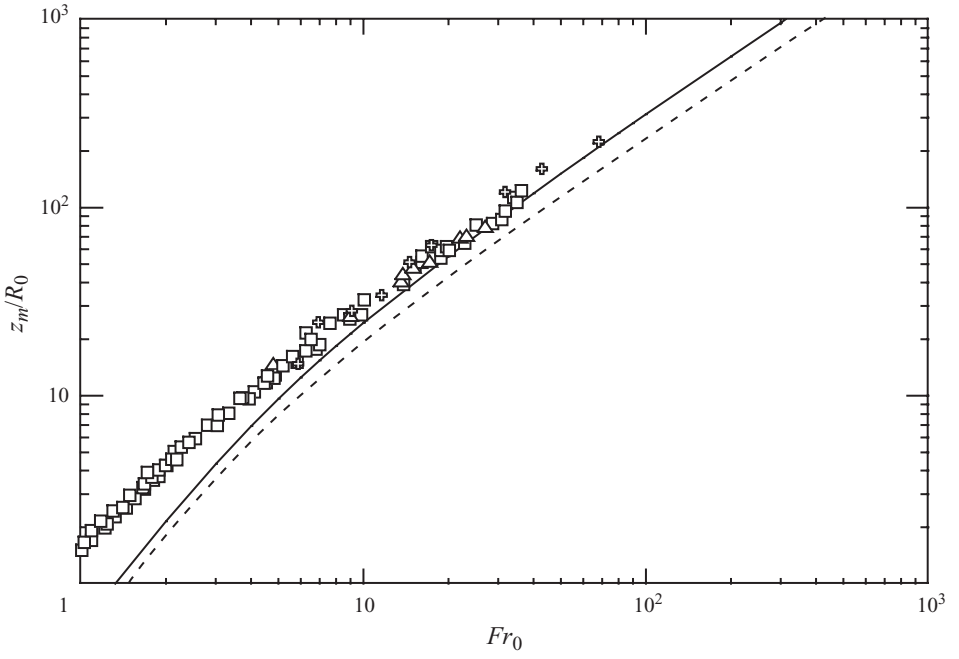

FIGURE 3. Comparison of experimental dimensionless maximum heights with the theoretical prediction using the model of Morton *et al.* (1956) together with $\alpha_e = 0.1$ (dotted line) and with the formalism of Kaminski *et al.* (2005) (solid line) for a 'top-hat' flow at the source. The symbols are the same as in figure 1.

jets and negatively buoyant jets or pure plumes). In the following, we will use the formula given in Carazzo *et al.* (2006) and Carazzo, Kaminski & Tait (2008*b*) to compute the value of A and thus the entrainment coefficient.

Figure 3 shows the comparison of experimental data with the theoretical predictions of the classical top-hat model (defined in (2.1)–(2.3)) together with the formalism of variable entrainment (defined in (3.1)–(3.3)). The predictions are improved at large Fr_0 but the discrepancy at small Fr_0 is not corrected. However, as it is experimentally difficult to vary the Froude number independently of the Reynolds number, turbulent fountains are often generated with intermediate Reynolds number at the source. It is thus likely that turbulence is not fully developed there. In that case the velocity profile at the nozzle may be intermediate between a Poiseuille flow and a top-hat. This will in turn change the relationship between the mass flux and the source momentum flux that becomes $M_0 = (4/3)\pi W_0^2 R_0^2$ for Poiseuille flow (Woods & Caulfield 1992).

Figure 4 shows that the experimental data are in good agreement with the theoretical predictions of the classical top-hat model together with our formalism, suggesting that for the most part they fall between laminar and turbulent exit conditions. For $Fr_0 > 20$ the fully turbulent model is satisfactory, but for lower Fr_0 the model with laminar exit conditions gives a better prediction, as expected. At intermediate Froude number, there is a transition zone in which one would expect the momentum flux at the source to be a function of the source geometry. For example, Mi, Nobes & Nathan (2001) presented experimental measurements of velocity profiles in the near field of jets issuing either from a smooth contraction pipe or from a long straight pipe. They showed that the development of the turbulence is enhanced when the source

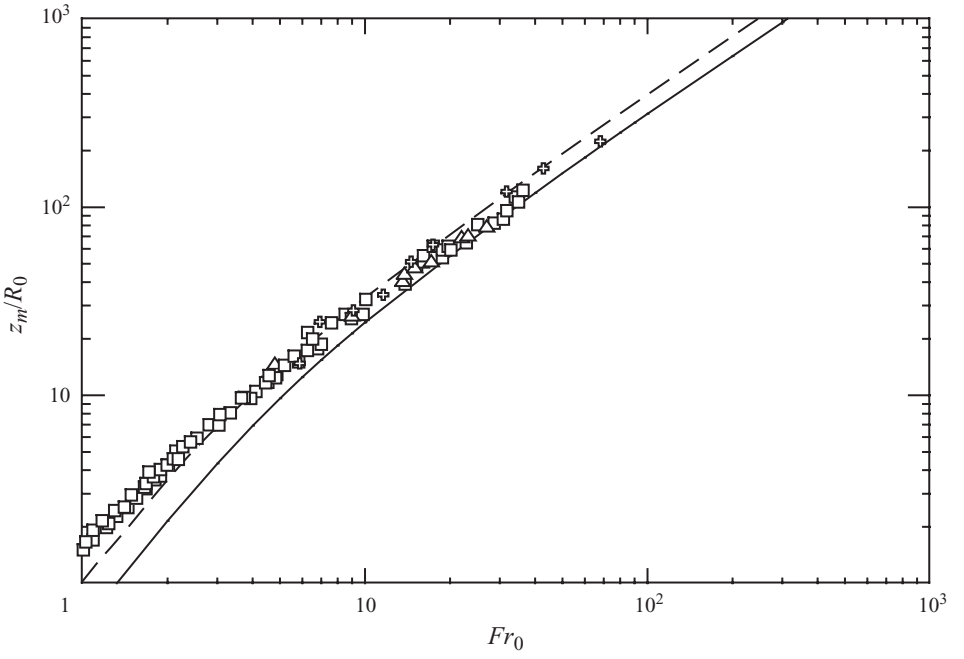

FIGURE 4. Comparison of experimental dimensionless maximum heights with the theoretical prediction using the model of Morton *et al.* (1956) together with the formalism of Kaminski *et al.* (2005) for a Poiseuille flow (dashed line) and a 'top-hat' flow (solid line) at the source. The symbols are the same as in figure 1.

nozzle is a smooth contraction pipe whereas the velocity profile becomes similar to a Poiseuille flow when the pipe is straight. Note that for $Fr_0 < 2$ the fountains are in the hydraulic regime described in Kaye & Hunt (2006), for which the formalism of turbulent entrainment no longer applies.

We thus conclude that the Morton *et al.* (1956) top-hat model provides good quantitative predictions for the initial rise of a turbulent fountain, as long as the effect of buoyancy on entrainment and the turbulence state at the source are taken into account. The exit conditions of fountains should be carefully investigated when studying the dynamics of these flows to further refine the predictions as a function of the nozzle geometry and Reynolds number at the source.

4. Steady-state height: a new 'confined' top-hat model

4.1. *Evolution of the steady-state height of a fountain as a function of the Froude number*

The steady-state height reached by a turbulent fountain is usually calculated by using the prediction of the initial maximum height corrected with the factor z_m/z_{ss} assumed constant at 1.43. Although the discrepancy between theoretical predictions and experimental data of maximum heights can be corrected once variable entrainment is taken into account, predictions for steady-state fountains can be affected by variations of z_m/z_{ss}.

Turner (1966) presented experiments that consisted in injecting dense jets of salty water upwards in a tank of fresh water. The results showed that the ratio of the initial rise height to the steady-state rise height varies within narrow limits with a

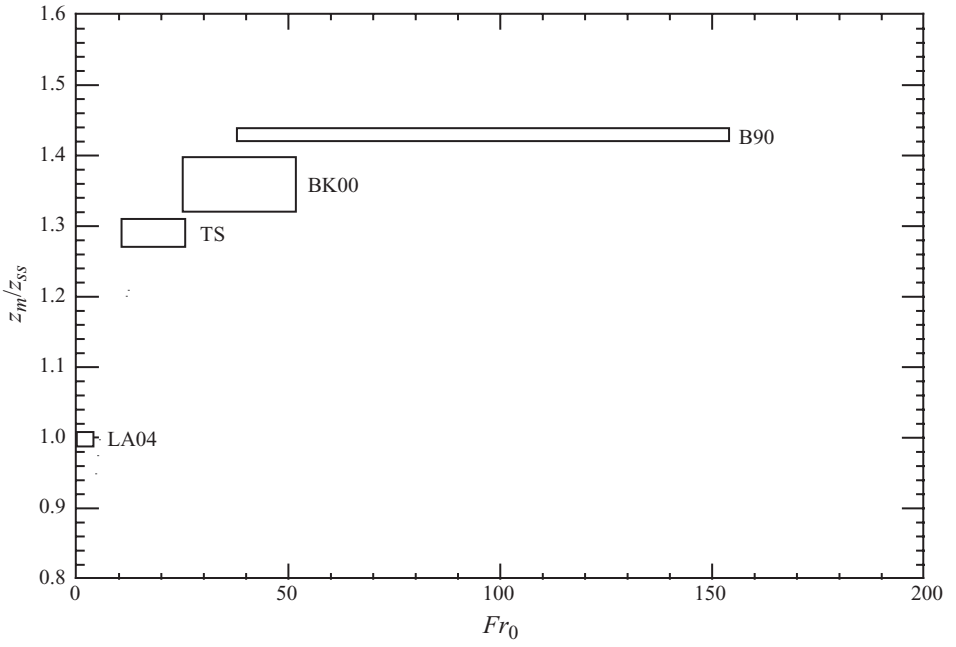

FIGURE 5. Ratio z_m/z_{ss} as a function of the source Froude number for a set of laboratory experiments and numerical simulations. LA04: Lin & Armfield (2004); TS, the present study (see the Appendix); BK00, Bloomfield & Kerr (2000); B90, Baines *et al.* (1990) (including the experiments of Turner 1966).

mean value of 1.43. Baines *et al.* (1990) extended this work up to an input Froude number of 250 and confirmed that $z_m/z_{ss} \approx 1.43$. However, Bloomfield & Kerr (2000) used a similar apparatus to generate fountains at $10 < Fr_0 < 70$ and found the ratio z_m/z_{ss} to be 1.36 ± 0.04. For low- and very low-Froude-number fountains, numerical solutions of Lin & Armfield (2004) show that the ratio z_m/z_{ss} is close to 1. We complemented this set of constraints by performing our own experiments using the apparatus described in Kaminski *et al.* (2005) to inject jets of fresh water downwards into a tank of salty water (details are given in the Appendix). The source Froude numbers varied between $5 < Fr_0 < 70$ and the mean value of the ratio of the initial to the final rise height over all the experiments was found to be 1.29 ± 0.02. Figure 5 summarizes the different values of z_m/z_{ss} we estimated from the literature and from our experiments and shows that this ratio systematically increases as a function of the source Froude number. Such a variation cannot be accounted for by the above model of a negatively buoyant turbulent starting jet and requires the modelling of the fully developed fountain, i.e. with an up-flow and a down-flow. To our knowledge, this systematic variation of z_m/z_{ss} with Fr_0 has not yet been discussed properly.

Previous studies tried to adapt the model of Morton *et al.* (1956) to turbulent fountains by setting out descriptions of both the up-flow and the surrounding down-flow at any height above the source. Such a full treatment involves many variables to describe the different couplings between the up-flow and down-flow, related to mass and momentum flux exchanges and to the effect of the relative buoyancy forces.

In the pioneering work of McDougall (1981) the entrainment rate of the down-flow into the up-flow is assumed to be proportional to the relative velocity $(W_u + W_d)$, where the subscripts 'u' and 'd' denote the up-flow and the down-flow as proposed by

Morton (1962) for coaxial plumes. On the other hand, the entrainment rates from the up-flow and from the environment into the down-flow are taken as proportional to the down-flow velocity W_d. Two sets of conservation equations of volume, momentum and buoyancy fluxes are written down, based on two different assumptions about how the buoyancy forces accelerate the up-flow (either as a function of the local difference between the up-flow and the down-flow density, or as a function of the density difference between the up-flow and the environment). Bloomfield & Kerr (2000) later showed that the two formulations lead to only 2.5 % of difference in the predictions of the steady-state height. Bloomfield & Kerr (2000) proposed an alternative theory that introduces four different formulations to estimate the steady-state height of a turbulent fountain. The predictions of these formulations strongly depend on the values of the entrainment coefficient between the down-flow and the environment and on the two entrainment coefficients between the up-flow and the down-flow whose uncertainties lead to drastic variations (up to 33 %) in the predictions of z_{ss}.

To gain better insight into the dynamics of the interaction between the up-flow and the down-flow in a turbulent fountain, we propose a simplified model that does not require the precise characterization of the down-flow. Using arguments of self-similarity of the flow, we also intend to obtain a better constrained model than in the more complete model of Bloomfield & Kerr (2000), which is somewhat difficult to comprehend.

4.2. *A confined 'top-hat' model*

As in Kaminski *et al.* (2005), we first write down mass, momentum and buoyancy conservation for a ring-shaped volume of an axisymetrical turbulent buoyant jet, under the Boussinesq approximation and steady state,

$$\frac{\partial}{\partial z}(r\overline{w}) + \frac{\partial}{\partial r}(r\overline{u}) = 0, \tag{4.1}$$

$$\frac{\partial}{\partial z}(r\overline{w}^2) + \frac{\partial}{\partial r}(r\overline{u}\,\overline{w}) = r\overline{g'} - \frac{\partial}{\partial r}(r\overline{\tilde{u}\tilde{w}}), \tag{4.2}$$

$$\frac{\partial}{\partial z}\left(r\overline{w}\overline{g'}\right) + \frac{\partial}{\partial r}\left(r\overline{u}\overline{g'}\right) = 0, \tag{4.3}$$

where r is the distance from the axis, u the radial velocity, w the vertical velocity and g' the reduced gravity. All quantities relate to mean values for the ring obtained by Reynolds averaging, and we neglect all contributions from turbulent fluctuations in velocity and reduced gravity that are of second order. The turbulent shear stress $-\rho\overline{\tilde{u}\tilde{w}}$ (which drives entrainment) is of leading order.

We then integrate these equations from $r=0$ to $r=\delta$, the boundary between the up-flow and the down-flow. We take as boundary condition $\overline{w}(r=\delta)=0$ as the vertical velocity changes sign between the up-flow and the down-flow. Note that the values of $\overline{u}(r=\delta)=u_\delta$, $\overline{\tilde{u}\tilde{w}}(r=\delta)=\tau_\delta$ and $\overline{g'}(r=\delta)=g'_\delta$ are not zero (Cresswell & Szczepura 1993) and not known *a priori*. The integration yields

$$\frac{\mathrm{d}}{\mathrm{d}z}\int_0^\delta r\overline{w}\,\mathrm{d}r = -\delta u_\delta, \tag{4.4}$$

$$\frac{\mathrm{d}}{\mathrm{d}z}\int_0^\delta r\overline{w}^2\,\mathrm{d}r = \int_0^\delta r\overline{g'}\,\mathrm{d}r - \delta\tau_\delta, \tag{4.5}$$

$$\frac{\mathrm{d}}{\mathrm{d}z}\int_0^\delta r\overline{w}\overline{g'}\,\mathrm{d}r = -\delta u_\delta g'_\delta. \tag{4.6}$$

Some information is required on the boundary conditions at $r=\delta$ to solve these conservation equations. One way to proceed is to replace the boundary conditions at $r=\delta$ by integral profiles, as in Kaminski *et al.* (2005). To do so, we construct additional conservation equations for quantities involving $\overline{w}$, namely the kinetic energy of axial motion, $(\overline{w}^2/2)$, the product $\overline{w}\overline{g'}$ and $\overline{w}^3$, which all cancel at $r=\delta$:

$$\frac{\partial}{\partial z}\left(r\overline{w}^3\right)+\frac{\partial}{\partial r}\left(r\overline{u}\,\overline{w}^2\right)=2r\overline{w}\overline{g'}-2\overline{w}\frac{\partial}{\partial r}\left(r\overline{\tilde{u}\tilde{w}}\right), \tag{4.7}$$

$$\frac{\partial}{\partial z}\left(r\overline{w}^2\overline{g'}\right)+\frac{\partial}{\partial r}\left(r\overline{u}\,\overline{w}\overline{g'}\right)=r\overline{g'}^2-\overline{g'}\frac{\partial}{\partial r}\left(r\overline{\tilde{u}\tilde{w}}\right), \tag{4.8}$$

$$\frac{\partial}{\partial z}(r\overline{w}^4)+\frac{\partial}{\partial r}\left(r\overline{u}\,\overline{w}^3\right)=3r\overline{w}^2\overline{g'}-3\overline{w}\frac{\partial}{\partial r}\left(r\overline{\tilde{u}\tilde{w}}\right). \tag{4.9}$$

The integration of the new conservation equations between $r=0$ and $r=\delta$ yields

$$\frac{\mathrm{d}}{\mathrm{d}z}\int_0^\delta r\overline{w}^3\,\mathrm{d}r=\int_0^\delta 2r\overline{w}\overline{g'}\,\mathrm{d}r-\int_0^\delta 2\overline{w}\frac{\partial}{\partial r}\left(r\overline{\tilde{u}\tilde{w}}\right)\,\mathrm{d}r, \tag{4.10}$$

$$\frac{\mathrm{d}}{\mathrm{d}z}\int_0^\delta r\overline{w}^2\overline{g'}\,\mathrm{d}r=\int_0^\delta r\overline{g'}^2\,\mathrm{d}r-\int_0^\delta \overline{g'}\frac{\partial}{\partial r}\left(r\overline{\tilde{u}\tilde{w}}\right)\,\mathrm{d}r, \tag{4.11}$$

$$\frac{\mathrm{d}}{\mathrm{d}z}\int_0^\delta r\overline{w}^4\,\mathrm{d}r=\int_0^\delta 3r\overline{w}^2\overline{g'}\,\mathrm{d}r-\int_0^\delta 3\overline{w}^2\frac{\partial}{\partial r}\left(r\overline{\tilde{u}\tilde{w}}\right)\,\mathrm{d}r. \tag{4.12}$$

We then use the three shape functions

$$\overline{w}(r,z)=w_m(z)\;f(r,z), \tag{4.13}$$

$$\overline{g'}(r,z)=g'_m(z)\;h(r,z), \tag{4.14}$$

$$\overline{\tilde{u}\tilde{w}}(r,z)=\tfrac{1}{2}w_m(z)^2\;j(r,z), \tag{4.15}$$

which define six dimensionless integral profiles,

$$I_1=\int_0^1 r^*f(r^*,z)h(r^*,z)\,\mathrm{d}r^*, \tag{4.16}$$

$$I_2=\int_0^1 f(r^*,z)\frac{\partial}{\partial r^*}[r^*j(r^*,z)]\,\mathrm{d}r^*, \tag{4.17}$$

$$I_3=\int_0^1 r^*h(r^*,z)^2\,\mathrm{d}r^*, \tag{4.18}$$

$$I_4=\int_0^1 h(r^*,z)\frac{\partial}{\partial r^*}[r^*j(r^*,z)]\,\mathrm{d}r^*, \tag{4.19}$$

$$I_5=\int_0^1 r^*f(r^*,z)^2h(r^*,z)\,\mathrm{d}r^*, \tag{4.20}$$

$$I_6=\int_0^1 f(r^*,z)^2\frac{\partial}{\partial r^*}[r^*j(r^*,z)]\,\mathrm{d}r^*, \tag{4.21}$$

with $r^*=r/\delta$. Last, the fluxes are written using a top-hat notation,

$$R^2W^3=a\int_0^\delta r\overline{w}^3\,\mathrm{d}r, \tag{4.22}$$

$$R^2W^4=b\int_0^\delta r\overline{w}^4\,\mathrm{d}r, \tag{4.23}$$

$$R^2W^2G' = c\int_0^{\delta} r\overline{w}^2\overline{g'}\,\mathrm{d}r, \tag{4.24}$$

where a, b and c are normalization constants to be defined later.

In the hypothesis of full self-similarity of the confined flow (i.e. profiles of velocity, buoyancy and turbulent shear stress are of similar form at all distances from the source), the shape functions do not depend on z and the conservation equations read

$$\frac{\mathrm{d}}{\mathrm{d}z}R^2W^3 = 2aR^2WG'I_1 + aRW^3I_2, \tag{4.25}$$

$$\frac{\mathrm{d}}{\mathrm{d}z}R^2W^4 = 3bR^2W^2G'I_5 + \frac{3}{2}bRW^4I_6, \tag{4.26}$$

$$\frac{\mathrm{d}}{\mathrm{d}z}R^2WG' = cR^2G'^2I_3 + \frac{1}{2}cRW^2G'I_4. \tag{4.27}$$

The hypothesis of self-similarity of the profiles could be relaxed to consider self-similarity drift as in Kaminski *et al.* (2005). We will see however that the agreement between model predictions and experimental data does not require such a detailed treatment for now. From the previous equations one may deduce the conservation equations for the (top-hat) mass, momentum and buoyancy fluxes,

$$\frac{\mathrm{d}}{\mathrm{d}z}R^2W = 2RW\left[\frac{3}{2}(aI_2 - bI_6) + \mathrm{sign}(G')\frac{3(aI_1 - bI_5)}{Fr^2}\right], \tag{4.28}$$

$$\frac{\mathrm{d}}{\mathrm{d}z}R^2W^2 = R^2G'\left[(4aI_1 - 3bI_5) + \mathrm{sign}(G')\left(2aI_2 - \frac{3b}{2}I_6\right)Fr^2\right], \tag{4.29}$$

$$\frac{\mathrm{d}}{\mathrm{d}z}R^2WG' = \frac{R^2G'^2}{W}(cI_3 + 2aI_1 - 3bI_5) + RWG'\left(\frac{c}{4}I_4 + aI_2 - \frac{b}{2}I_6\right), \tag{4.30}$$

where $Fr = W/\sqrt{R|G'|}$ is the local Froude number. The question of the choice of the normalization constants a, b and c has been discussed by Fox (1970) and Morton (1971) for a non-buoyant jet, and by Kaminski *et al.* (2005) for a jet with arbitrary buoyancy. For the present case of a turbulent fountain, we choose these constants first to recover a conservation equation of momentum flux identical to the one used in the formalism by Morton *et al.* (1956), $a = (3bI_6)/4I_2 = (1 - 3bI_5)/4I_1$. We then impose the additional condition $c = -bI_6/I_4$, which yields

$$\frac{\mathrm{d}}{\mathrm{d}z}R^2W = 2RW\left[\frac{C_f}{2} - \mathrm{sign}(G')\left(1 - \frac{1}{A_f}\right)\frac{1}{Fr^2}\right], \tag{4.31}$$

$$\frac{\mathrm{d}}{\mathrm{d}z}R^2W^2 = R^2G', \tag{4.32}$$

$$\frac{\mathrm{d}}{\mathrm{d}z}R^2WG' = kR^2WS, \tag{4.33}$$

where

$$S = \frac{G'^2}{W^2} \tag{4.34}$$

has the same dimensions as a stratification parameter (Carazzo *et al.* 2008*b*). This set of equations is similar but not identical to the one used in our previous studies (Kaminski *et al.* 2005; Carazzo *et al.* 2006, 2008*b*). C_f, A_f and k are combinations

of the integral profiles and emerge as the key parameters governing the model:

$$C_f = \frac{I_2 I_6}{4(I_2 I_5 - I_1 I_6)}, \tag{4.35}$$

$$A_f = \frac{4(I_1 I_6 - I_2 I_5)}{7 I_1 I_6 - 8 I_2 I_5}, \tag{4.36}$$

$$k = 1 + \frac{3 I_1 I_4 I_6 + 2 I_2 I_3 I_6}{6(I_2 I_4 I_5 - I_1 I_4 I_6)}. \tag{4.37}$$

In this 'confined' top-hat formalism, the mass conservation equation gives an explicit expression for the entrainment coefficient,

$$\alpha_e \equiv \frac{C_f}{2} - \mathrm{sign}(G') \left(1 - \frac{1}{A_f}\right) \frac{1}{Fr^2}, \tag{4.38}$$

whereas the conservation equation of buoyancy flux involves a coefficient k quantifying the buoyancy transfer between the up- and down-flows. Although other choices for the normalization constants a, b and c would have led to slightly different sets of equations equally valid mathematically, the conditions we retained allow a clear interpretation of the dynamics of a steady-state fountain. Because the down-flow entrains fluid from the environment, the up-flow is surrounded by a stratified environment. Contrary to the classical case of a buoyant plume rising into an environment whose density is decreasing with the distance from the source, the confined up-flow is rising into an environment whose density is increasing with the distance from the source. Thus, the negative buoyancy flux should increase towards zero (i.e. become less negative) as a function of increasing z. This statement requires that $k > 0$. Exact analytical expressions for the various integral parameters are presently out of reach. We thus used the laboratory measurements of velocity, buoyancy and turbulent shear stress profiles made by Cresswell & Szczepura (1993) to evaluate the six integrals and hence to estimate our three governing parameters (figure 6). We obtain that $C_f = 0.170 \pm 0.040$, $A_f = 0.244 \pm 0.086$ and $k = 8.4 \pm 3.5$. Figure 7 shows the predictions of our confined top-hat model for the steady-state heights using the values inferred from Cresswell & Szczepura (1993). Although good agreement between the theoretical predictions and experimental results is observed at low and intermediate Froude numbers, a discrepancy remains for large Froude numbers. One may note that the experiment of Cresswell & Szczepura (1993) was performed at low Froude number (i.e. $Fr_0 = 3.2$) for which our new model provides satisfying predictions of steady-state height. The discrepancy at large Froude numbers could be interpreted as an evolution of the dynamic similarity of the flow as a function of the distance from the source (Carazzo *et al.* 2006). As the uncertainties on the values of C_f, A_f and k are quite large, $\sim$24 %, $\sim$35 % and $\sim$42 %, respectively, we investigate the effect of their variations by performing a sensitivity analysis.

The complexity of the explicit expression for C_f, A_f and k make their precise interpretation quite difficult. Some insight can be gained by considering the evolution of the set of equations when buoyancy becomes negligible, i.e. when $Fr \to \infty$. At very large Froude number, the influence on the down-flow will tend to vanish and the 'confined' top-hat will tend to mimic the evolution of a pure jet ($Fr \to \infty$). In that case, C_f will be equivalent to the entrainment coefficient for pure jets, i.e. the parameter C defined in Kaminski *et al.* (2005) and introduced previously here in (3.1) and (3.3). We thus consider that C_f quantifies the fraction of kinetic energy in the flow available for turbulent entrainment. A sensitivity analysis of this parameter within

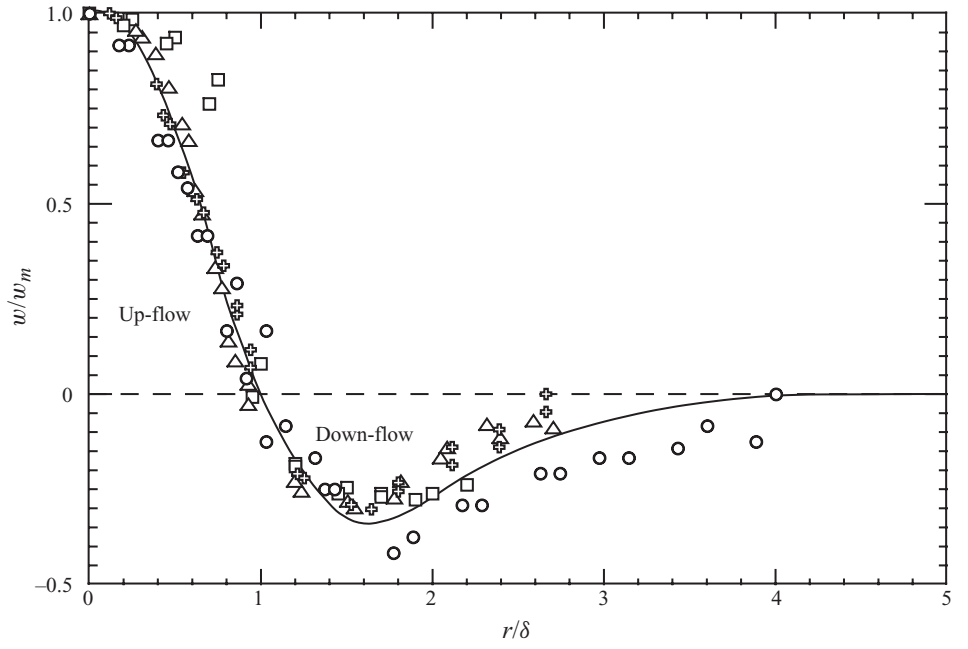

FIGURE 6. Radial profiles of the mean vertical velocity (up-flow, $w/w_m > 0$; down-flow, $w/w_m < 0$), measured by Cresswell & Szczepura (1993) at $z/R_0 = 0$ (□), $z/R_0 = 2$ (△), $z/R_0 = 4$ (✣) and $z/R_0 = 6$ (○). The solid line gives the best fit profile.

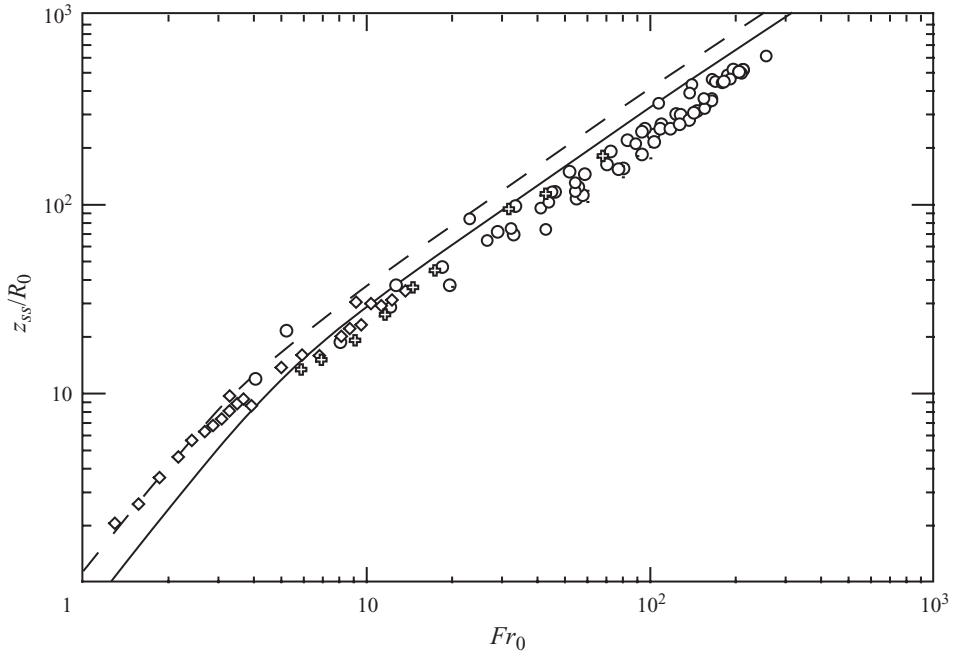

FIGURE 7. Comparison of experimental dimensionless steady-state heights with the theoretical prediction using our new model with $C_f = 0.170$, $A_f = 0.244$ and $k = 8.4$ for a Poiseuille flow (dashed line) and a 'top-hat' flow (solid line) at the source. The symbols are the same as in figure 2.

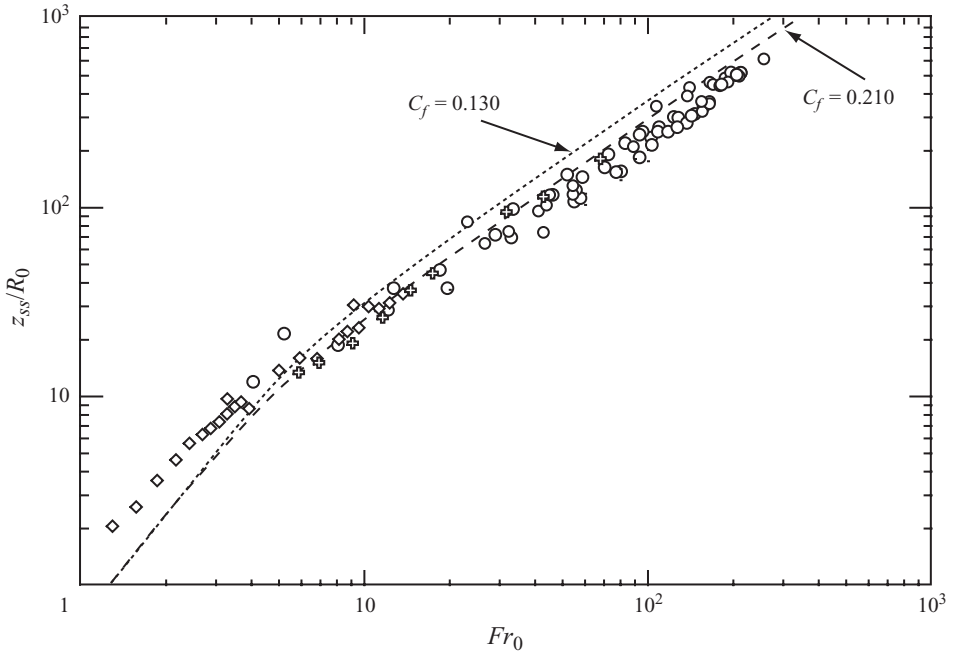

FIGURE 8. Comparison of experimental dimensionless steady-state heights with the theoretical prediction using our new model with $C_f = 0.210$, $A_f = 0.244$ and $k = 8.4$ (dashed line), $C_f = 0.130$, $A_f = 0.244$ and $k = 8.4$ (dotted line) for a 'top-hat' flow at the source. The symbols are the same as in figure 2.

the error bars reveals that its exact value does not strongly influence the theoretical predictions (figure 8). For the present purpose, we therefore use $C_f = 0.170$ as a universal constant.

By analogy with the formalism introduced in Kaminski *et al.* (2005), we also propose that A_f encompasses the influence of the relative shapes of velocity, buoyancy and turbulent stress profiles on the transfer of gravitational energy to turbulent stress. The difference between A_f and the parameter A introduced in Kaminski *et al.* (2005) and in (3.1) and (3.2) is an explicit dependence of A_f on the turbulent shear stress profile, whereas A depends only on the velocity and buoyancy profiles. This can be interpreted to reflect stronger coupling between the flow variables in the up-flow due to the 'confinement' of the profiles by the down-flow at $r = \delta$. The positive value of A_f implies that negative buoyancy reduces entrainment, as in Kaminski *et al.* (2005). As for C_f, a sensitivity analysis of A_f shows that this parameter only slightly influences theoretical predictions (figure 9). For the present purpose, we therefore choose the value deduced from the literature $A_f = 0.244$ as a universal constant.

The interpretation of k is more difficult. The positive value obtained is consistent with the gain of buoyancy flux due to the entrainment of some fluid from the down-flow whose density is increasing with the distance from the source (i.e. decreasing from the steady-state height due to mixing with environmental fluid). One might have expected that a full description of the down-flow would be necessary in order to quantify the buoyancy changes induced in the up-flow by mixing with the down-flow. Based on the hypothesis of a self-similar flow, our confined top-hat model does not however require such a treatment: the effect of the down-flow is encompassed in

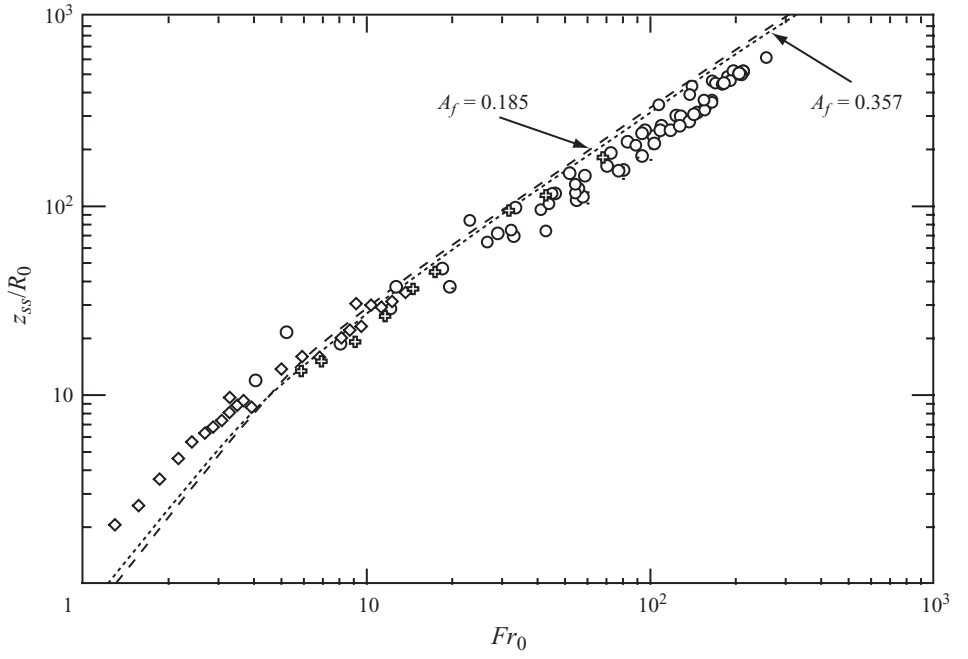

FIGURE 9. Comparison of experimental dimensionless steady-state heights with the theoretical prediction using our new model with $C_f = 0.170$, $A_f = 0.185$ and $k = 8.4$ (dashed line), $C_f = 0.170$, $A_f = 0.357$ and $k = 8.4$ (dotted line) for a 'top-hat' flow at the source. The symbols are the same as in figure 2.

the constant k whose value reflects the confinement of the profiles by the downflow. Figure 10 suggests however that the value of k strongly influences theoretical predictions, and shows that good agreement between the model and the measurements can be obtained at large Froude numbers for values of k towards the upper bound of the error bar. In the absence of experimental constraints on k at large distance from the source, we assume that this parameter may slightly evolve from a value in the lower bound of the error bar to another one in the upper bound as a function of the downstream distance from the source.

Figure 11 shows the predictions of our confined top-hat model for the steady-state height of a turbulent fountain as a function of the source Froude number. The agreement between theoretical predictions – based on the average values of A_f, C_f deduced from the literature and best fit values for k ranging within those obtained from the integral profiles – and the experimental results at different Froude numbers, validate the approach, and in particular the hypothesis of self-similarity. Beyond an improved quantitative prediction of z_{ss}, our new formulation provides a qualitative interpretation of the origin of the variation of z_m/z_{ss} as a function of the Froude number. During the initial rise, the flow behaves like a negatively buoyant jet and the maximum height scales with $\alpha_m^{-1/2} M_0^{3/4} B_0^{-1/2}$ (Turner 1966), where $B_0 = |g_0'| W_0 R_0^2$ is the source (positive) buoyancy flux. In the steady-state regime, the following dimensional argument $z_{ss} \sim \alpha_{ss}^{-1/2} B_0^{1/4} S^{-3/8}$ can be used to reduce (4.31)–(4.33) to their simplest non-dimensional form, in the same manner as Morton *et al.* (1956) for buoyant plumes rising in a stratified environment. Replacing S in terms of source fluxes ($= B_0^2/M_0^2$),

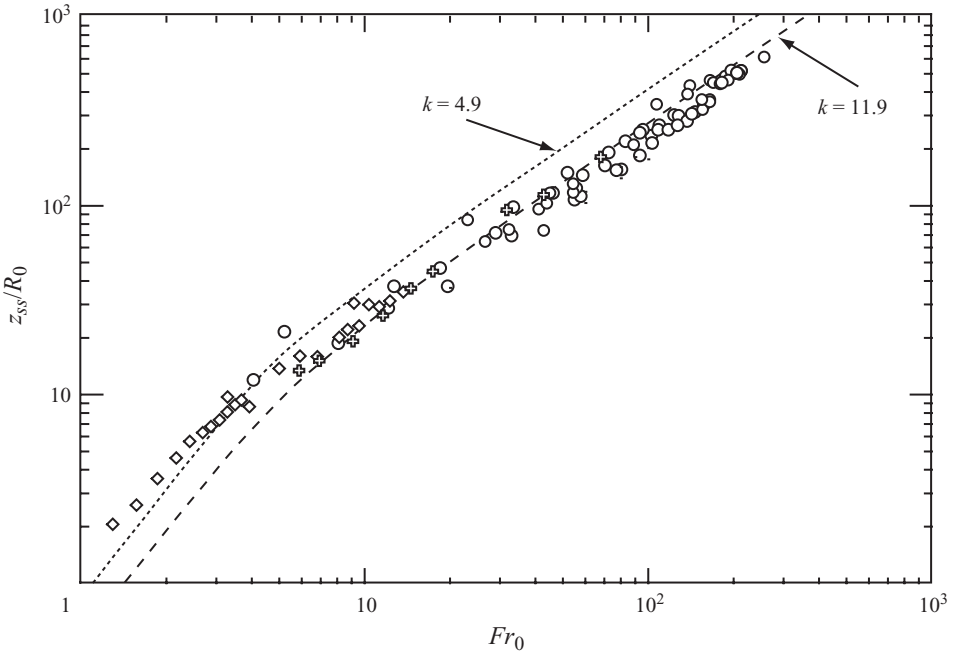

FIGURE 10. Comparison of experimental dimensionless steady-state heights with the theoretical prediction using our new model with $C_f = 0.170$, $A_f = 0.244$ and $k = 11.9$ (dashed line), $C_f = 0.170$, $A_f = 0.244$ and $k = 4.9$ (dotted line) for a 'top-hat' flow at the source. The symbols are the same as in figure 2.

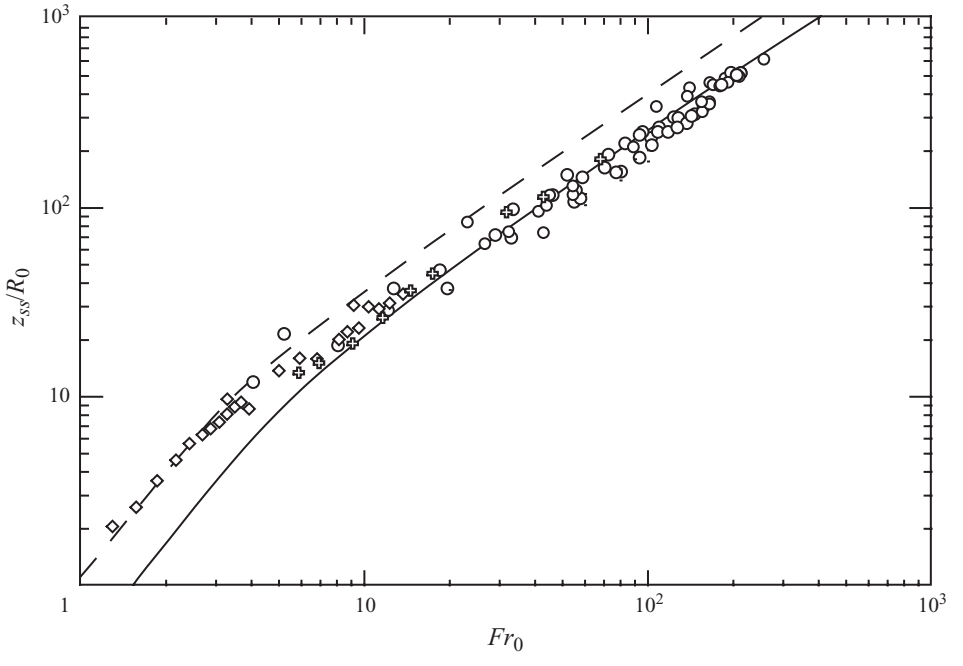

FIGURE 11. Comparison of experimental dimensionless steady-state heights with the theoretical prediction using our new model with $C_f = 0.170$, $A_f = 0.244$ and the value of k that best fits the data, $k = 8$ for a Poiseuille flow (dashed line) and $k = 14$ for a 'top-hat' flow (solid line) at the source. The symbols are the same as in figure 2.

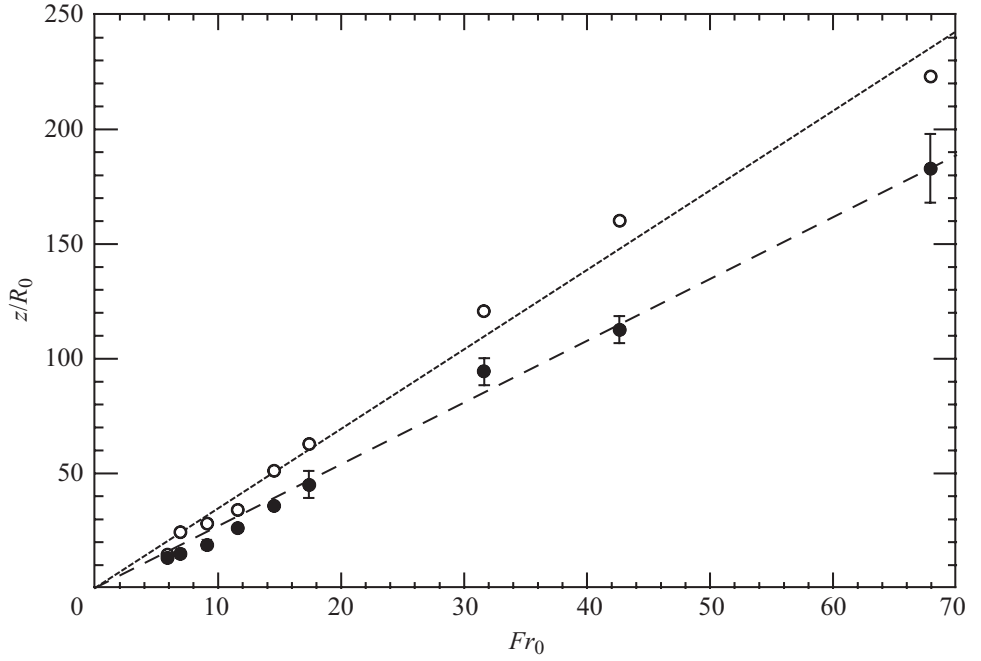

FIGURE 12. Laboratory measurements of maximum (○) and steady-state (●) fountain heights as a function of the source Froude number. Dotted and dashed lines correspond to linear best fits for maximum and steady-state heights, respectively. The ratio of the slopes of the dotted and dashed lines gives a value for z_m/z_{ss} of 1.29 ± 0.02.

the ratio z_m/z_{ss} scales with

$$\frac{z_m}{z_{ss}} \propto \sqrt{\frac{\alpha_{ss}}{\alpha_m}}, \tag{4.39}$$

where α_m and α_{ss} are the values of the entrainment coefficient during the initial stage (defined in (3.1)) and for the steady-state regime (defined in (4.38)), respectively. For highly forced fountains, for which Fr tends to infinity (or $Ri \to 0$), α_{ss} tends to C_f and α_m tends to C. As C_f is larger than C, entrainment is larger in steady-state fountains, leading to a smaller height for the fountain (i.e. $z_m > z_{ss}$), as observed. For very weak fountains, for which Fr tends to 0 (or $Ri \to \infty$), entrainment is much reduced (i.e. α_{ss} and $\alpha_m \sim 0$), and the height depends only on the initial parameter (Kaye & Hunt 2006), which yields $z_m = z_{ss}$, as observed.

5. Conclusions

In order to achieve a better quantitative prediction of the dynamics of turbulent fountains as a function of their source Froude number, we propose a new top-hat model for the initial rise and steady-state behaviour of axisymmetrical fountains. Good agreement between the model and the experimental data on the initial rise of the fountains is achieved only when taking into account two refinements of the classical Morton *et al.* (1956) model: (i) the reduction of the entrainment process as a function of increasing negative buoyancy, and (ii) the influence of the source Reynolds number on the effective momentum flux at the source. For the case of steady-state fountains, previous models required the calculation of both the central up-flow and of

Experiment	R_0 (cm)	Q_0 ($g\,s^{-1}$)	W_0 ($m\,s^{-1}$)	g'_0 ($m\,s^{-2}$)	z_m/R_0 –	z_m/R_0 –	Fr –	Re –
1	0.455	18.3	0.28	0.36	24.6	15.0	6.7	1280
2	0.455	24.0	0.37	0.36	28.3	19.0	9.1	1680
3	0.455	30.6	0.47	0.36	34.2	26.3	11.6	2145
4	0.2	2.1	0.17	0.41	14.8	13.3	5.9	335
5	0.2	5.2	0.41	0.41	51.3	36.0	14.5	830
6	0.1	2.7	0.86	0.41	160.3	112.7	42.6	860
7	0.1	2.0	0.64	0.41	120.9	94.8	31.6	640
8	0.1	1.1	0.35	0.41	63.0	45.1	17.4	350
9	0.1	4.3	1.37	0.41	223.2	183.0	67.9	1370

TABLE 1. Experimental conditions at the source and measured heights. $Q_0 = \rho_0 \pi W_0 R_0^2$ is the source mass flux, with $\rho_0 = 998.0\,kg\,m^{-3}$ for all the experiments.

the annular down-flow, with the introduction of many free parameters. We developed instead a 'confined' version of the top-hat formalism that allows the calculation of the down-flow without an explicit characterization of the down-flow. The effect of the down-flow is described by the parameter k whose value is constrained by experimentally measured profiles. More careful laboratory measurements on profiles, including turbulent shear stress which is often omitted (Mizushina *et al.* 1982), will help to better constrain the key parameters of the model and their possible evolution to a state of self-similarity. The new model presented in this paper allows a good fit of experimental data and explains the systematic decrease of the ratio between the initial and steady-state heights of fountains with increasing Froude number in terms of the evolution of entrainment as a function of buoyancy.

G. Carazzo was supported by CIFAR, NSERC and a PIMS post-doctoral fellowship (CRG on Geophysical and Complex Fluid Dynamics). The contribution of E. Kaminski and S. Tait to this work is IPGP contribution 2616.

Appendix. Laboratory experiments

The measurements of laboratory fountain heights used here have been obtained using the experimental apparatus described in Kaminski *et al.* (2005). A turbulent jet of fresh water was injected downwards into a 45 cm × 45 cm × 45 cm tank containing salt water of varying density. The flow rate was controlled with a valve and measured using a weighing machine and a timer. The source fresh water was injected through a constriction copper pipe with varying inner radii (0.1, 0.2 and 0.455 cm). The 'collapse' of the fountain to the top of the tank was filmed using a video camera in order to measure the initial and the steady-state fountain heights (figure 12). The conditions and measurements for each experiment are given in table 1.

REFERENCES

ANSONG, J. K., KYBA, P. J. & SUTHERLAND, B. R. 2008 Fountains impinging on a density interface. *J. Fluid. Mech.* **595**, 115–139.

BAINES, W. D., TURNER, J. S. & CAMPBELL, I. H. 1990 Turbulent fountains in an open chamber. *J. Fluid. Mech.* **212**, 557–592.

BLOOMFIELD, L. J. & KERR, R. C. 2000 A theoretical model of a turbulent fountain. *J. Fluid. Mech.* **424**, 197–216.

Branney, M. J. & Kokelaar, P. 1992 Pyroclastic density currents and the sedimentation of ignimbrites. *Geol. Soc. Mem.* **27**.

Campbell, I. H. & Turner, J. S. 1989 Fountains in magma chambers. *J. Petrol.* **30**, 885–923.

Carazzo, G., Kaminski, E. & Tait, S. 2006 The route to self-similarity in turbulent jets and plumes. *J. Fluid. Mech.* **547**, 137–148.

Carazzo, G., Kaminski, E. & Tait, S. 2008*a* On the dynamics of volcanic columns: a comparison of field data with a new model of negatively buoyant jets. *J. Volcanol. Geotherm. Res.* **178**, 94–103.

Carazzo, G., Kaminski, E. & Tait, S. 2008*b* On the rise of turbulent plumes: quantitative effects of variable entrainment for submarine hydrothermal vents, terrestrial and extra terrestrial explosive volcanism. *J. Geophys. Res.* **113**, B09201.

Cotel, A. J., Gjestvang, J. A., Ramkhelawan, N. N. & Breidenthal, R. E. 1997 Laboratory experiments of a jet impinging on a stratified interface. *Exp. Fluids* **23**, 155–160.

Cresswell, R. W. & Szczepura, R. T. 1993 Experimental investigation into a turbulent jet with negative buoyancy. *Phys. Fluids* **11**, 2865–2878.

Fox, D. G. 1970 Forced plume in a stratified fluid. *J. Geophys. Res.* **33**, 6818–6835.

Friedman, P. D. 2006 Oscillation height of a negatively buoyant jet. *ASME J: J. Fluids Engng* **128**, 880–882.

Friedman, P. D., Vadakoot, V. D., Meyer, W. J. & Carey, S. 2007 Instability threshold of a negatively buoyant fountain. *Exp. Fluids* **42**, 751–759.

Hunt, G. R. & Coffey, C. J. 2009 Characterising line fountains *J. Fluid. Mech.* **623**, 317–327.

Hunt, G. R. & Kaye, N. B. 2005 Lazy plumes. *J. Fluid. Mech.* **533**, 329–338.

Kaminski, E., Tait, S. & Carazzo, G. 2005 Turbulent entrainment in jets with arbitrary buoyancy. *J. Fluid. Mech.* **526**, 361–376.

Kaye, N. B. & Hunt, G. R. 2006 Weak fountains. *J. Fluid. Mech.* **558**, 319–328.

Koh, R. C. Y. & Brooks, N. H. 1975 Fluid mechanics of waste-water disposal in the ocean. *Annu. Rev. Fluid Mech.* **7**, 187–211.

Lin, W. & Armfield, S. W. 2000*a* Direct simulation of weak axisymmetric fountains in a homogeneous fluid. *J. Fluid. Mech.* **403**, 67–88.

Lin, W. & Armfield, S. W. 2000*b* Very weak axisymmetric fountains in a homogeneous fluid. *Numer. Heat Transfer* **38**, 377–389.

Lin, W. & Armfield, S. W. 2003 The Reynolds and Prandtl number dependence of weak fountains. *Comput. Mech.* **31**, 379–389.

Lin, W. & Armfield, S. W. 2004 Direct simulation of fountains with intermediate Froude and Reynolds numbers. *ANZIAM J.* **45**, 66–77.

Lin, W. & Armfield, S. W. 2008 Onset of entrainment in transitional round fountains. *Intl J. Heat Mass Trans.* **51**, 5226–5237.

Lin, Y. J. P. & Linden, P. F. 2005 The entrainment due to a turbulent fountain at a density interface. *J. Fluid. Mech.* **542**, 25–52.

Linden, P. F. 2000 Convection in the environment. In *Perspectives in Fluid Dynamics* (ed. G. K. Batchelor, H. K. Moffatt & M. G. Worster), pp. 287–343. Cambridge University Press.

McDougall, T. J. 1981 Negatively buoyant vertical jets. *Tellus* **33**, 313–320.

Mi, J., Nobes, D. S. & Nathan, G. J. 2001 Influence of jet exit conditions on the passive scalar field of an axisymmetric free jet. *J. Fluid. Mech.* **432**, 91–125.

Mizushina, T., Ogino, F., Takeuchi, H. & Ikawa, H. 1982 An experimental study of vertical turbulent jet with negative buoyancy. *Wärme Stoffübertrag.* **16**, 15–21.

Morton, B. R. 1959 Forced plumes. *J. Fluid. Mech.* **5**, 151–163.

Morton, B. R. 1962 Coaxial turbulent jets. *J. Heat Mass Transfer* **5**, 955–965.

Morton, B. R., Taylor, G. I. & Turner, J. S. 1956 Turbulent gravitational convection from maintained and instantaneous source. *Proc. R. Soc. Lond.* **234**, 1–23.

Morton, G. I. 1971 The choice of conservation equations for plume models. *J. Geophys. Res.* **30**, 7409–7416.

Papanicolaou, P. N., Papakonstantis, I. G. & Christodoulou, G. C. 2008 On the entrainment coefficient in negatively buoyant jets. *J. Fluid. Mech.* **614**, 447–470.

Philippe, P., Raufaste, C., Kurowski, P. & Petitjeans, P. 2005 Penetration of a negatively buoyant jet in a miscible liquid. *Phys. Fluids* **17**, 053601.

Turner, J. S. 1966 Jets and plumes with negative or reversing buoyancy. *J. Fluid. Mech.* **26**, 779–792.

Williamson, N., Srinarayana, N., Armfield, S. W., McBain, G. D. & Lin, W. 2008 Low-Reynolds-number fountain behaviour. *J. Fluid. Mech.* **608**, 297–317.

Woods, A. W. & Caulfield, C. P. 1992 A laboratory study of explosive volcanic eruptions. *J. Geophys. Res.* **97**, 6699–6712.

Zhang, H. & Baddour, R. E. 1997 Maximum vertical penetration of plane turbulent negatively buoyant jets. *J. Engng Mech.* **123**, 973–977.

Zhang, H. & Baddour, R. E. 1998 Maximum penetration of vertical round dense jets at small and large Froude numbers. *J. Hydraul. Engng* **124**, 550–553.